Perovskite-derived $MnO_x/LaMnO_3$ Nanocomposites to boost CO oxidation activity

Supplementary Information

Andrea Felli[a], Alessandra Toso[a], Andrea Braga[a], Sara Colussi[a], Marta Boaro[a], Jordi Llorca[b], Byron Truscott[c], Christine Artner-Wallner[c], and Alessandro Trovarelli[a*]

a. Polytechnic Department, University of Udine, Via del Cotonificio 108, 33100, Udine (Italy)

b. Institute of Energy Technologies and Department of Chemical Engineering, Universitat Politècnica de Catalunya, EEBE, Eduard Maristany 10-14, 08019, Barcelona (Spain).

c. Treibacher Industrie AG, Auer-von-Welsbach-Straße 1, 9330, Althofen (Austria)

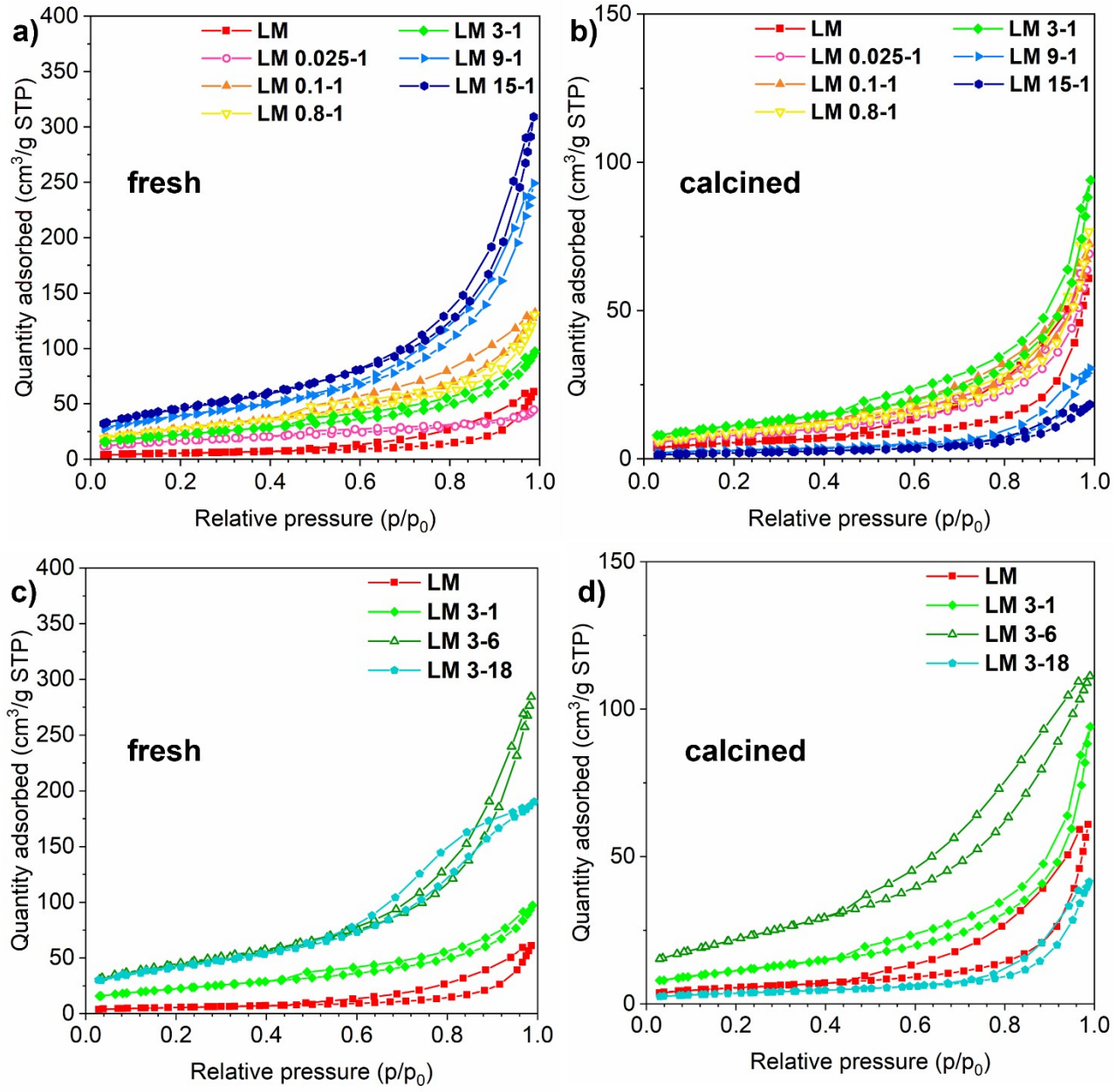

Fig. S1. N_2 adsorption/desorption isotherms for: 1a) fresh LM samples (i.e. after the acid treatment) treated with different acid concentrations; in 1b) the corresponding calcined samples (i. e. after a calcination of 1 hour at 823 K in static air); in 1c) fresh LM samples treated by variation the duration of the treatment; in 1d) the corresponding calcined samples.

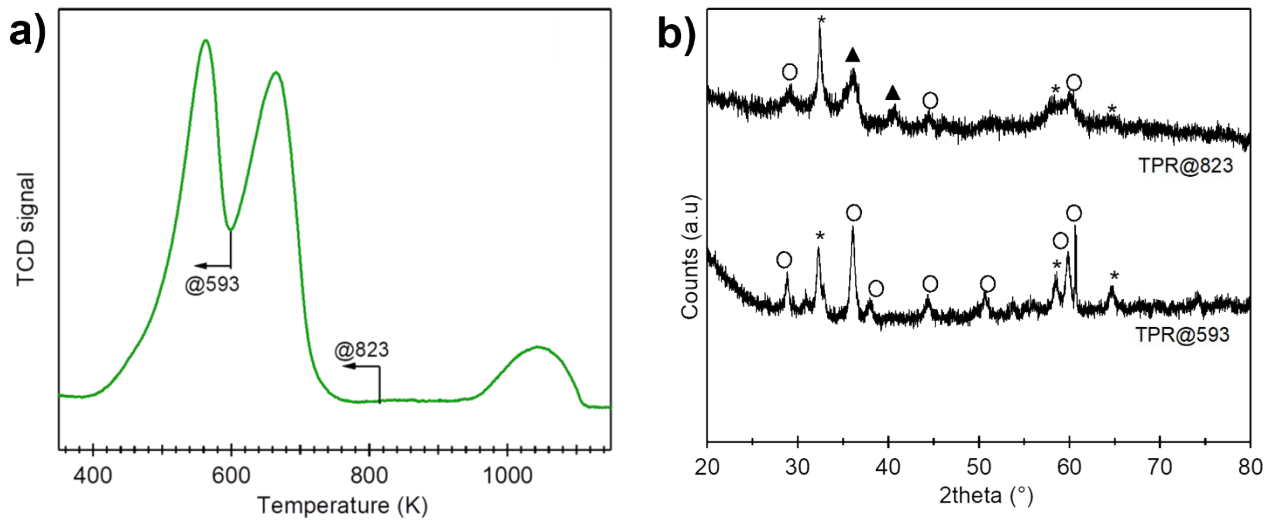

Fig. S2. (a) TPR of LM 3-6. Arrows indicate the collection points for XRD analysis during the heating ramp; (b) XRD patterns of LM 3-6 stop@593 and stop@823 during H_2-TPR. * $LaMnO_3$, ○ Mn_3O_4, ▲ MnO.

Two TPR experiments were carried out on LM 3-6. In the first one, we stopped the heating ramp during the TPR at 593 K. while the second experiment was stopped at 823 K. By looking at the XRD acquired on the spent materials, it is possible to see that the first reduction peak led to the formation of Mn_3O_4 while the second reduction resulted in the formation of a mixture of Mn_3O_4 and MnO. Therefore, based on the XRD results, the first peak can be attributed to the reduction of MnO_2 and Mn_2O_3 to Mn_3O_4 (TPR@593), which is then reduced to MnO in concomitance with the second peak (TPR@823).

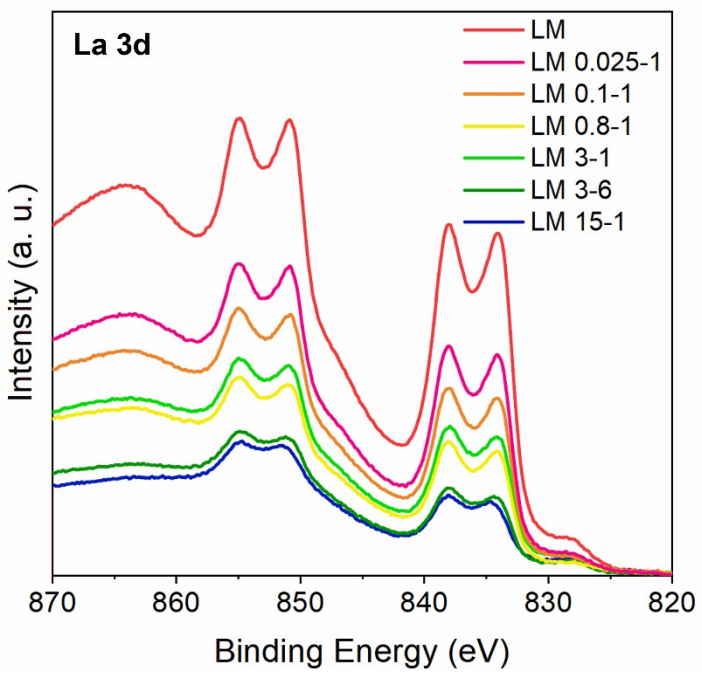

Figure S3: La 3d spectra of LM samples.

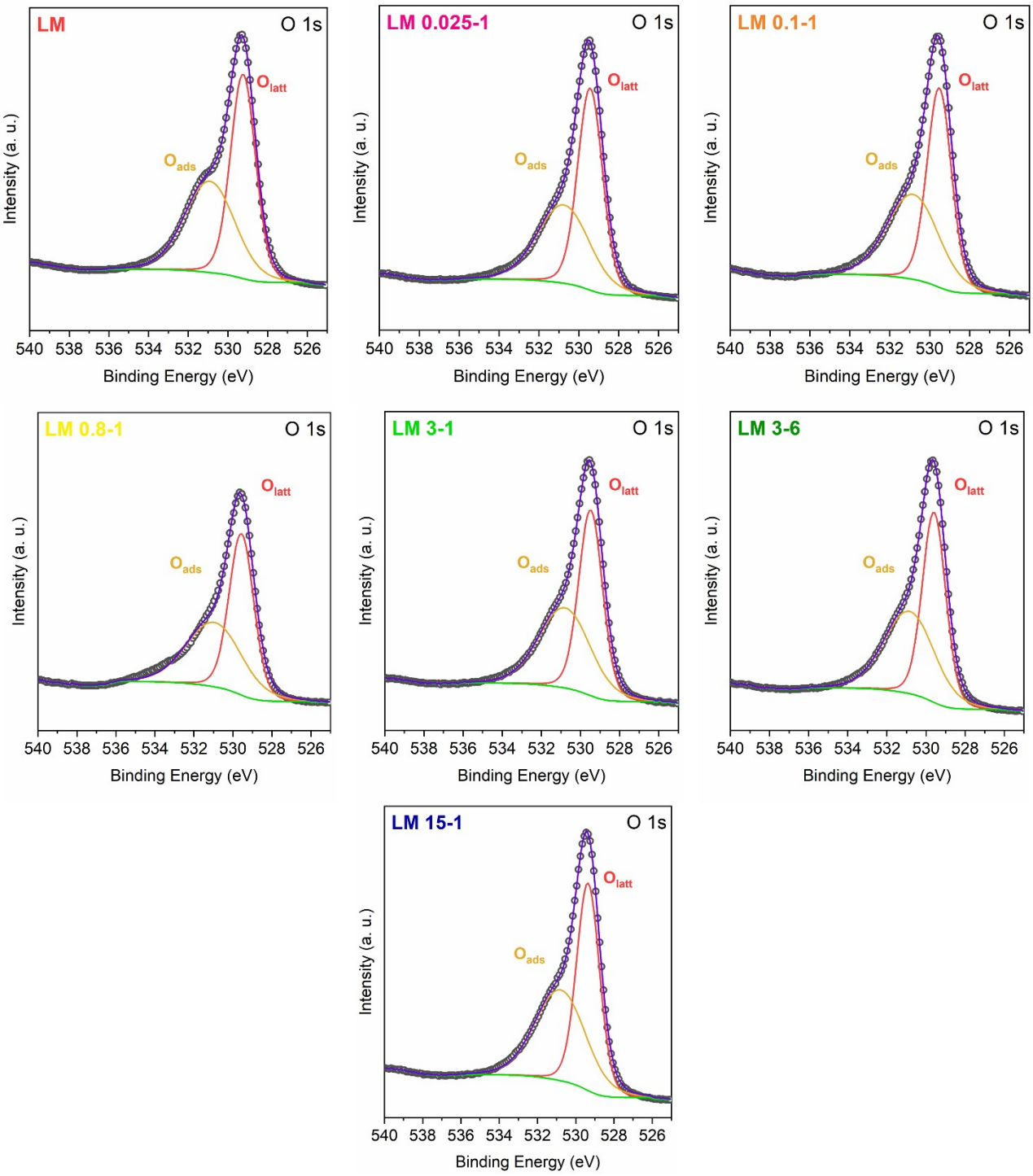

Figure S4: O 1s spectra and fitting of LM samples.

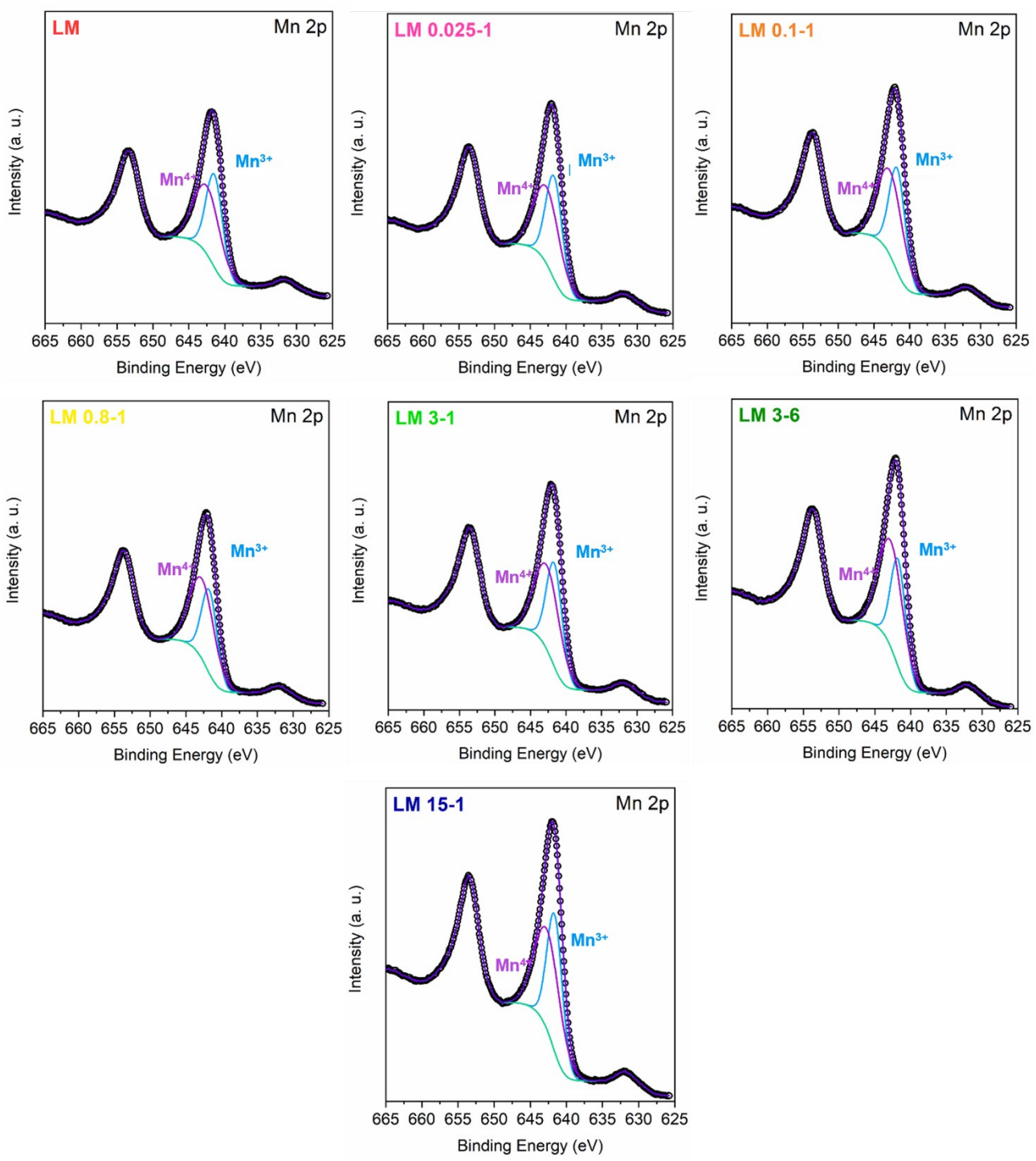

Figure S5: Mn 2p spectra and fitting of LM samples.

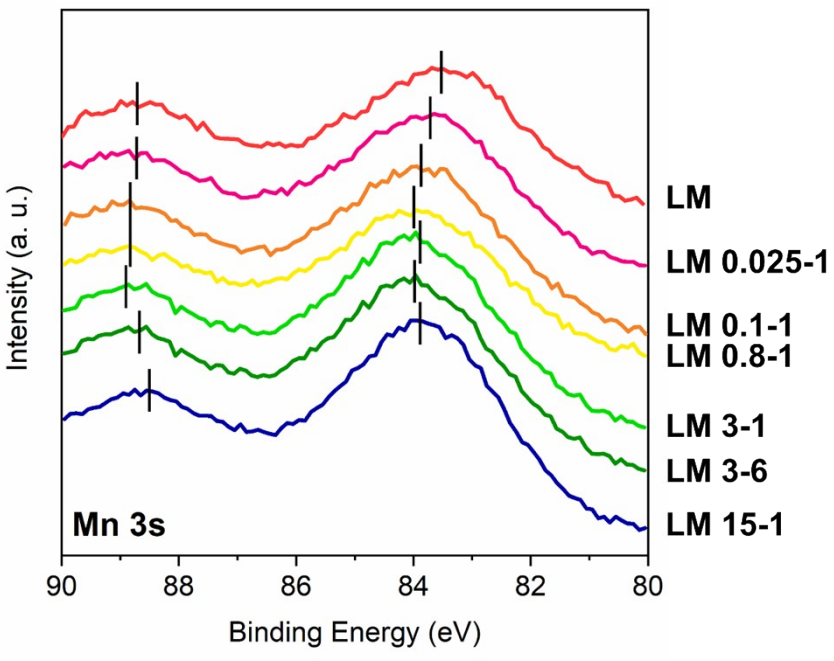

Figure S6: Mn 3s splitting spectra and evaluation of ΔE_{3s}.

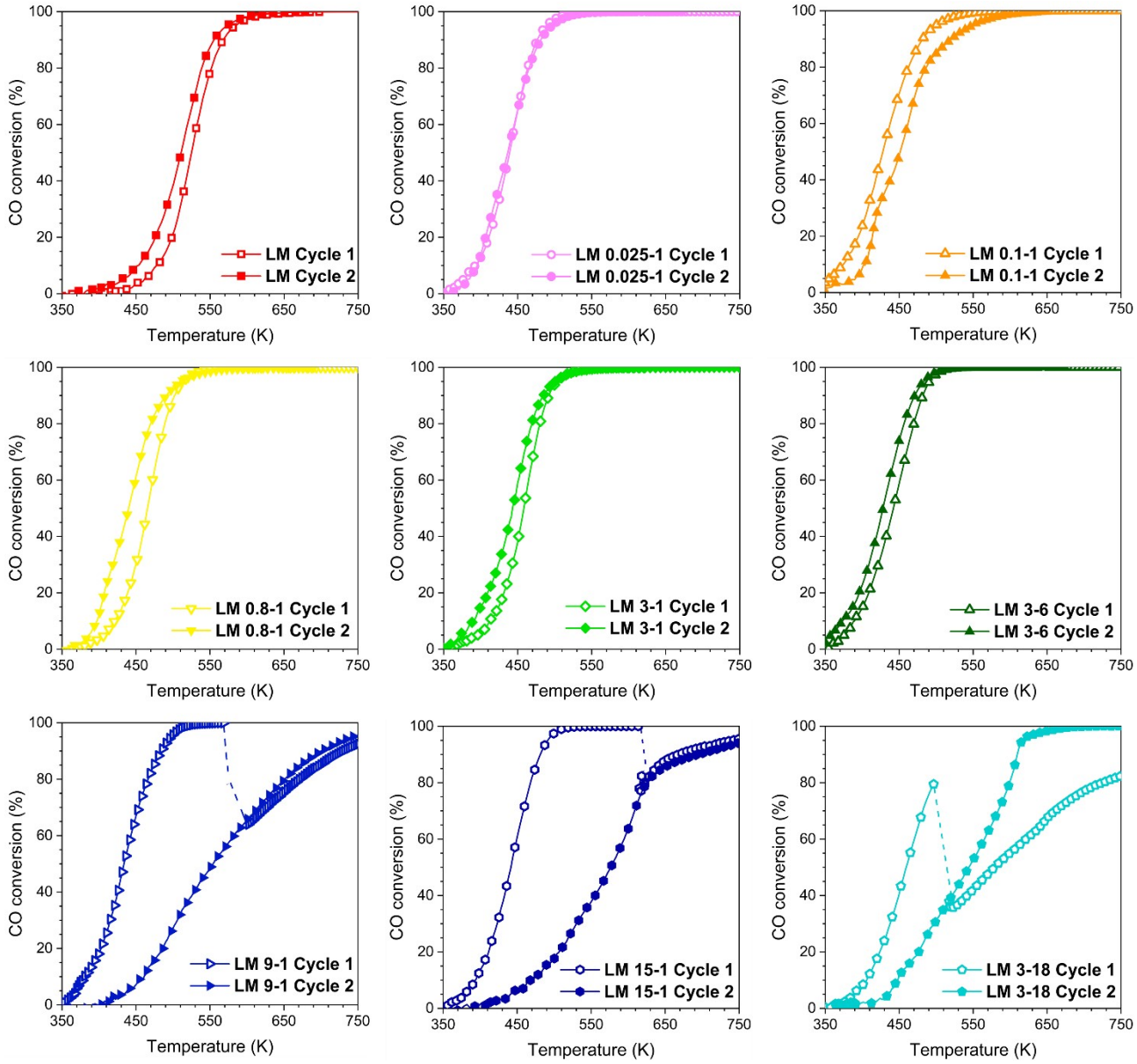

Figure S7: Catalytic activity of LM samples during two consecutive CO oxidation cycles.

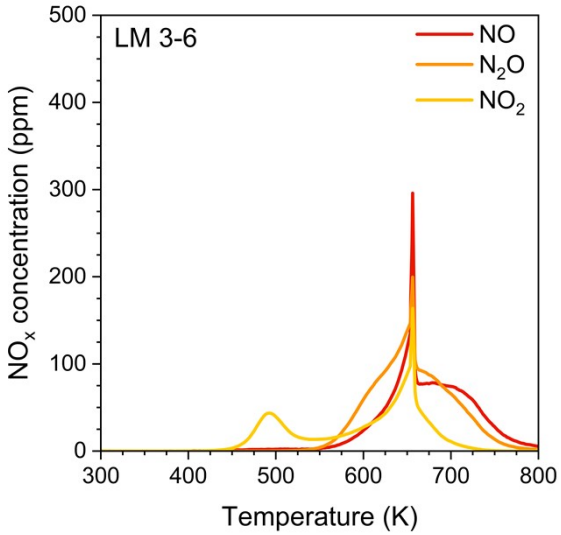

Figure S8 NO_x release during the first catalytic cycle of LM 3-6.

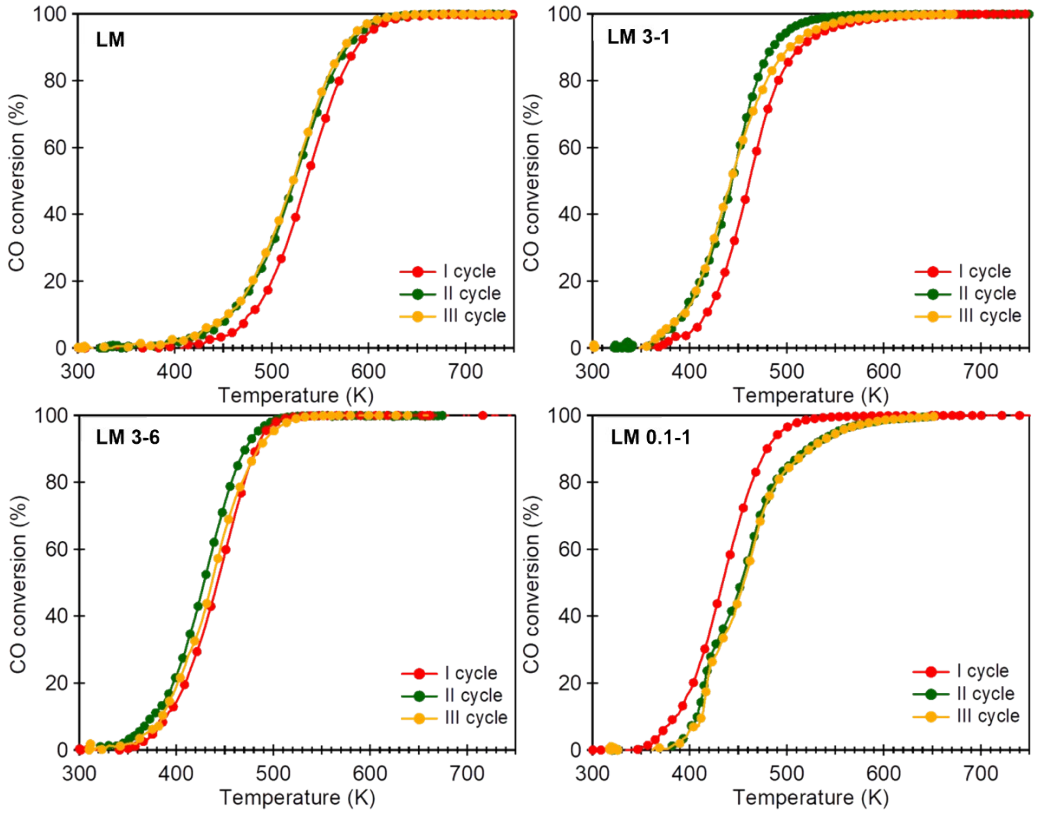

Figure S9. Catalytic activity of LM, LM 0.1-1, LM 3-1, and LM 3-6 during three consecutive CO oxidation cycles.

Table S1: BET surface area of the most representative fresh, calcined and used catalysts.

Sample name	Fresh BET SA (m^2/g)	Calcined BET SA (m^2/g)	Used BET SA (m^2/g)
LM	20	/	22
LM 3-1	80	40	44
LM 3-6	158	80	71
LM 9-1	138	10	12
LM 15-1	165	7	12

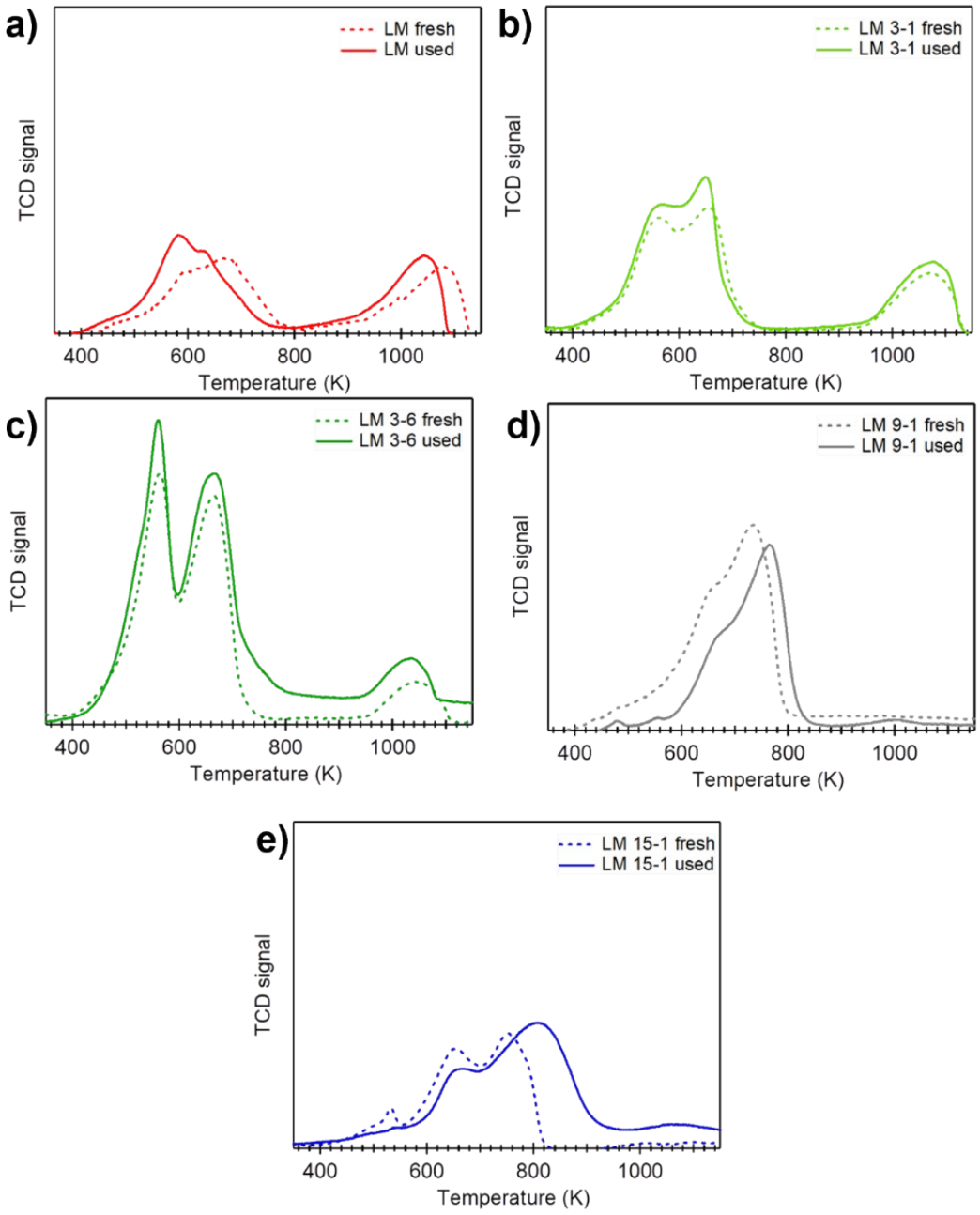

Figure S10. H_2-TPR profile of the used LM, LM 3-1, LM 3-6, LM 6-1, LM 9-1 and LM 15-1 (after CO oxidation test).

Table S2. Comparison with some catalysts from the literature.

Sample	CO:O_2 ratio	Flow rate (mL/min)	Gas composition	GHSV ($mL \cdot g^{-1} \cdot h^{-1}$)	T_{50} (K)	Ref.
LM	1:10	300	1% CO, 10% O_2, 89% N_2	90000	520	This work
LM 0.025-1	1:10	300	1% CO, 10% O_2, 89% N_2	90000	436	This work
LM 3-6	1:10	300	1% CO, 10% O_2, 89% N_2	90000	429	This work
$LaFeO_3$	1:20	400	1% CO, 20% O_2, 79% He	12000	621	1
$LaCo_{0.9}O_3$	2:10	80	2% CO, 10% O_2, 88% N_2	120000	493	2
$LaNiO_3$	0.1:5	100	0.1% CO, 5% O_2, 94.9% N_2	60000	421	3
γ-MnO_2	1:20	102.5	1% CO, 20% O_2, 79% N_2	30750	390	4
δ- MnO_2	1:20	102.5	1% CO, 20% O_2, 79% N_2	30750	508	4
α-MnO_2	1:20	102.5	1% CO, 20% O_2, 79% N_2	30750	573	4
β-MnO_2	1:20	102.5	1% CO, 20% O_2, 79% N_2	30750	726	4
$Ce_{0.67}Mn_{0.33}O_2$	1:5	100	1% CO, 5% O_2, 84% He	60000	414	5
$Mn_{0.83}Co_{0.17}O_x$	1:20	/	1% CO, 20% O_2, 79% N_2	/	453	6
Pt-TiO_2	1:16	400	1% CO, 16% O_2, 83% N_2	60000	371	7

1 P. Ciambelli, S. Cimino, S. De Rossi, L. Lisi, G. Minelli, P. Porta and G. Russo, *Appl Catal B*, 2001, **29**, 239–250.

2 M. Kim, J. H. Cho, K. Tae Park, C. Houn Rhee, H. Woong Park and J. Chul Jung, *Journal of Industrial and Engineering Chemistry*, 2024, **139**, 250–257.

3 L. Gan, P. Ye, X. Tian, Q. Wu, H. Shi, S. Xiong, J. Chen and J. Li, *Appl Surf Sci*, DOI:10.1016/j.apsusc.2024.162215.

4 J. Xu, T. Zhang, Y. Sun, S. Fang, Z. Wu, J. Zhu, L. Dai, W. Liu, B. Zhang, J. Zhang, S. Yao, E. Gao and J. Li, *Appl Catal A Gen*, DOI:10.1016/j.apcata.2023.119519.

5 M. V. Grabchenko, G. V. Mamontov, M. V. Chernykh, O. V. Vodyankina and M. A. Salaev, *Chem Eng Sci*, DOI:10.1016/j.ces.2023.119593.

6 O. A. Bulavchenko, T. N. Afonasenko, S. S. Sigaeva, A. V. Ivanchikova, A. A. Saraev, E. Y. Gerasimov, V. V. Kaichev and S. V. Tsybulya, *Top Catal*, 2020, **63**, 75–85.

7 T. Zhang, P. Zheng, J. Gao, X. Liu, Y. Ji, J. Tian, Y. Zou, Z. Sun, Q. Hu, G. Chen, W. Chen, X. Liu, Z. Zhong, G. Xu, T. Zhu and F. Su, *Nat Commun*, DOI:10.1038/s41467-024-50790-3.